Individual variability in behavior and functional networks predicts vulnerability using a predator scent model of PTSD

David Dopfel[#1], Pablo D. Perez[#1], Alexander Verbitsky[2], Hector Bravo-Rivera[3], Yuncong Ma[1], Gregory J. Quirk[3], Nanyin Zhang*[1]

[1]Department of Biomedical Engineering, Pennsylvania State University, University Park, PA, USA
[2]Department of Engineering Science and Mechanics, Pennsylvania State University, University Park, PA, USA
[3]Departments of Psychiatry and Anatomy & Neurobiology, University of Puerto Rico School of Medicine, San Juan, Puerto Rico

#: These authors contributed equally to this work.

***Address for correspondence:**

Nanyin Zhang, Ph.D

Professor of Biomedical Engineering and Electrical Engineering

The Huck Institutes of Life Sciences

The Pennsylvania State University

W-341 Millennium Science Complex, University Park, PA 16802, USA

Email: nuz2@psu.edu

Acknowledgments

The present study was partially supported by National Institute of Neurological Disorders and Stroke Grant R01NS085200 (PI: Nanyin Zhang, PhD) and National Institute of Mental Health Grant R01MH098003 and RF1MH114224 (PI: Nanyin Zhang, PhD) and R37MH058883 (PI: Gregory Quirk).

Conflict of interest: none.

Key words: Post-traumatic Stress Disorder; Vulnerability; Resilience; Rat; Resting-state fMRI

Abstract:

Only a minority of individuals who experience traumatic event(s) subsequently develop post-traumatic stress disorder (PTSD). However, whether differences in vulnerability to PTSD result from predisposition or a consequence of trauma exposure remains unclear. A major challenge in differentiating these possibilities is that clinical studies focus on individuals already exposed to traumatic experiences, and do not take into account pre-trauma conditions. Here using the predator scent model of PTSD in rats and a longitudinal design, we measured pre-trauma brain-wide neural circuit functional connectivity (FC), behavioral and corticosterone responses to trauma exposure, and post-trauma anxiety. Individual differences in freezing responses to predator scent exposure correlated with differences in pre-trauma FC in a set of neural circuits, especially in olfactory and stress-related systems, indicating that pre-existing function in these circuits could predispose animals to differential fearful responses to threats. Counterintuitively, rats with the lowest freezing showed more avoidance of the predator scent, a prolonged corticosterone response, and higher anxiety long after exposure. This study provides a comprehensive framework of pre-existing circuit function that determines threat response strategy, which might be directly related to the development of PTSD-like behaviors.

Introduction

Maladaptive response to trauma may lead to chronic stress disorders like posttraumatic stress disorder (PTSD). While trauma exposure is a feature of PTSD, it is not an unequivocal predictor of the disorder. In fact, only a minority of individuals who experience traumatic event(s) subsequently develop PTSD. However, mechanisms underlying this individual difference in vulnerability remain unclear.

It has been suggested that vulnerability to PTSD may result from individual differences in early life events, preexisting conditions, or responses to trauma exposure [1-3]. However, mixed results have been reported. For instance, reduced hippocampal volume has long been considered a marker of PTSD. Nevertheless, some studies suggest that PTSD-related decreases in hippocampal volume might be a consequence of traumatic events and PTSD development, whereas other studies showed that PTSD patients' twins who did not have a trauma experience also had smaller hippocampal volumes, suggesting that reduced hippocampal volume may pre-dispose individuals to developing PTSD [4-7]. These conflicting results are also reported in studies of cortisol levels and brain activity in relation to PTSD [8-10], which together contribute to our elusive understanding of individual vulnerability to PTSD.

A major obstacle of investigating risk factors of PTSD is rooted in the difficulty of longitudinally monitoring of PTSD development pre- through post-trauma in humans with well-controlled traumatic events. Studies in humans focus on populations already exposed to a variety of uncontrolled traumatic events [11]. Such barriers can be overcome in experimental animals, for which a longitudinal design with controlled traumatic stressors can be conveniently applied. Among many stress paradigms that have been

71 used to produce rat models of PTSD, predator scent exposure in an inescapable
72 environment is a commonly used psychological stressor [12]. This method mimics a life-
73 threatening situation that is ecologically relevant and physically innocuous, preventing
74 confounding effects of inflammation or pain due to injury. Recent work with this model
75 has found that PTSD-like behaviors are exhibited following exposure to predator scent [13].
76 Importantly, Cohen et al. distinguished the responses of mal- vs. well-adapted rats,
77 showing a 25-30% prevalence of PTSD-like behavior in rats exposed to trauma [14]. This
78 work highlights the potential for this animal model to investigate relevant individual
79 variability in PTSD-like responses to trauma. Missing from previous studies, however, is
80 information about preexisting conditions of animals that might predict their immediate and
81 long-term responses to trauma.

82 Additionally, little is known about whether and how specific defense responses to
83 a threat correlate with susceptibility to maladaptation. Exposure to a stressor elicits
84 different fear responses depending on the perceived proximity and intensity of the threat.
85 Moderate stressors produce passive freezing, while imminent predation threats elicit a
86 fight or flight response [15,16]. However, whether behavioral responses to predator scent is
87 a useful indicator of subsequent development of PTSD is unknown.

88 Here we employed a longitudinal approach to studying individual variability of
89 behavioral and functional outcomes of the predator scent animal model of PTSD. Resting-
90 state functional magnetic resonance imaging (rsfMRI) data were collected from awake
91 rodents before trauma exposure to record pre-existing neural circuit function using the
92 awake rat rsfMRI approach established in our lab [17-20]. Awake rat rsfMRI avoids
93 confounding factors from anesthetics and permits correlation with behavior [21-23]. We

found that individual differences in behavior and neural circuit function prior to trauma exposure predicted animals' susceptibility to developing PTSD-like behaviors. This suggests that pre-existing traits such as anterior olfactory nucleus (AON)-amygdala connectivity may be critical for determining individual resilience/susceptibility to developing PTSD.

Results

The experimental schedule was summarized in Fig. 1a. Rats were first scanned using rsfMRI, then exposed to fox urine, and then given an anxiety test approximately one week after exposure.

Freezing responses to fox urine were highly variable across animals

A total of 87 Long-Evans (LE) rats were exposed to a predator scent stressor in the form of a compressed cotton pad sprayed with fox urine in an inescapable cage for 10 min. Freezing and location within the cage were quantified with behavioral tracking software (ANY-maze, Stoelting Co., Reston, VA). Compared to control animals that were exposed to a clean cotton pad, the group exposed to predator scent showed increased freezing (t-test, $t_{87} = 3.660$, $p = 0.00044$, Fig. 1b, left), and maintained a significantly greater distance from the cotton pad (t-test, $t_{87} = 3.568$, $p = 0.00060$, Fig. 1b, right). These data confirm that predator scent exposed animals displayed a significantly greater stress response compared to controls.

Closer examination of animals' freezing time revealed distinct distributions between groups. Fig. 1c showed the histograms of freezing time in both groups. Control

116 animals exhibited a unimodal distribution of freezing, whereas predator scent exposed
117 animals displayed large inter-subject variability with a bimodal distribution (Fig. 1c, right
118 panel) fitted with a mixed Gaussian distribution (bimodal Gaussian function provided the
119 best fit relative to uni-modal and tri-modal Gaussian functions, model fit quality (the model
120 with the lowest AIC is the best model to fit the data): Δ_1(AIC) = 11, Δ_2(AIC) = 0, Δ_3(AIC)
121 = 6; Akaike weight for each model: w_1 = 0.0039, w_2 = 0.947, w_3 = 0.0488). To further
122 investigate this variation in freezing behavior, predator scent exposed animals in the top
123 and bottom tertiles of freezing time were separated into high-freezing and low-freezing
124 subgroups, respectively (n = 21 for each subgroup). Fig. 1d plotted freezing time as a
125 function of exposure time in high-freezing, low-freezing and control groups. Interestingly,
126 it was found that freezing differed between high- and low-freezing animals even during
127 the first minute of predator scent exposure (two sample t-test, $p < 0.009$) and this
128 difference became larger over the time course of exposure. There was no difference
129 between low-freezing rats and controls. There was also no significant difference in
130 mobility among all three groups, as evidenced by the maximum speed during exposure
131 (one-way ANOVA, $F_{(2, 62)} = 0.86$, $p = 0.43$, Supplement Fig. 1).

132

133 *Low-, but not high-freezing animals were susceptible to developing PTSD-like behaviors*

134 The fact that freezing time was almost identical between low-freezing and control
135 animals might suggest that low-freezing animals had a similar stress response to controls.
136 However, the spatial distribution of time spent in the cage during exposure suggested a
137 different interpretation (Fig. 2). Control animals did not show a side preference with a near
138 normal distribution of the time spent close to the center of the cage (Fig. 2a). In contrast,

both high and low freezing animals exhibited a leftward skewed distribution of time spent, farther away from the fox urine. The average distance from the cotton pad was significantly greater in both low- and high-freezing animals compared to controls (One-way ANOVA, $F_{(2, 62)} = 10.97$, $p = 0.000050$ and $p = 0.031$, respectively), indicating avoidance behavior in exposed animals. This difference was also supported by the normalized freezing time at different distances from the cotton pad, as shown in Fig. 2b. Similar to the distribution of the total time spent in the cage, control animals did not seem to have any preference for the side of the cage in which they froze, whereas both high- and low-freezing animals tended to freeze farther away from the fox urine sample. Relative to high-freezing animals, low-freezing animals showed even more leftward bias. The normalized freezing time was significantly less in the zone 24 cm away from the pad (Two-way Repeated ANOVA, $F_{Group \times Zone}(22, 682) = 3.00$, $p = 0.0000059$; Tukey-Kramer post-hoc test, low- vs high-freezing at 24 cm: $p = 0.04$), indicating that low-freezing animals were somewhat more avoidant than high-freezing animals. This can also be seen in the heat plots of Fig. 2a. Prior to predator scent exposure during the habituation period, the three groups showed no significant differences in freezing time (One-way ANOVA, $F_{Group \times Zone}(2, 62) = 0.24$, $p = 0.78$, Supplement Fig. 2) or location distribution (the cage was divided into three even-size zones, Two-way ANOVA, $F_{Group \times Zone}(4, 186) = 1.28$, $p = 0.28$).

To assess the long-lasting PTSD-like behaviors in exposed animals, we measured anxiety levels using an elevated-plus maze (EPM) 6 days after predator scent exposure. Resembling the observation of increased avoidance, low-freezing animals exhibited heightened long-lasting anxiety compared to both control (t-test, $t = 2.24$, $p = 0.030$) and

162 high-freezing animals (t-test, t = 3.37, p = 0.0017), as indicated by the ratio of
163 open/open+close arm time in EPM tests (Fig. 2c). There was no statistical difference
164 between high-freezing and control animals, indicating that low-, but not high-freezing
165 animals were susceptible to developing PTSD-like behaviors following exposure to
166 predator scent. In addition, freezing was positively correlated with the EPM score in
167 exposed animals (R^2 = 0.21, p = 0.0002), but not controls (R^2 = 0.01, p = 0.62, Fig. 2d).
168 These results demonstrate that behavioral responses during trauma exposure can predict
169 long-term maladaptation. Furthermore, in a separate experiment (Supplement Fig. 3) low-
170 freezing animals were also associated with other types of PTSD-like behaviors including
171 more marble burying behavior (n = 5 each group, two sample t-test, t = 5.47, p = 0.048),
172 less habituation to acoustic startle response (n = 9 each group, two-sample t-test, t = 5.3,
173 p = 0.050) and less pre-pulse inhibition (n = 9 each group, two-sample t-test, t = 5.16, p
174 = 0.037) than high-freezing animals 6 days post predator scent exposure. This provides
175 additional evidence that low-freezers were vulnerable to developing PTSD-like behaviors.

176

177 *Low-freezing animals showed prolonged corticosterone response to predator scent*

178 We also measured the corticosterone (CORT) level immediately before predator
179 scent exposure (0 min, baseline) as well as 30 min, 60 min and 120 min after exposure
180 (Fig. 3, 15 controls including 9 exposed to air and 6 exposed to lemon scent, as well as
181 24 fox urine exposed animals). Again, we grouped rats according to their freezing time
182 during predator scent exposure with 12 low-freezing and 12 high-freezing animals (we
183 did not use tertiles given a relatively smaller sample size in this experiment).

184 There was a significant difference in CORT level changes over time among groups
185 (Two-way repeated ANOVA, $F_{group \times time}$ (6,108) = 2.84, p = 0.023, Fig. 3a). In particular,
186 control animals showed no significant CORT change across time (One-way repeated
187 ANOVA, F_{time} (3,56) = 0.8, p = 0.50). High-freezing animals exhibited a relatively short
188 CORT response, peaking at 30 min and returning to baseline at 60 min (Tukey-Kramer
189 test, 30 min vs 60 min: p = 0.049; 0 min vs 60 min: p = 0.54; 60 min vs 120 min: p = 0.93).
190 The peak amplitude of CORT response at 30 min was comparable between high- and
191 low-freezing animals (Tukey-Kramer test, p = 0.59). However, relative to high-freezing
192 rats, the CORT response in low-freezing animals was prolonged, maintained at a high
193 level at 60 min (Tukey-Kramer test, 30 min vs 60 min: p = 1; 0 min vs 60 min: p = 0.0005)
194 and had a delayed return to baseline at 120 min (Tukey-Kramer test, 60 min vs 120 min:
195 p = 0.0098; 0 min vs 120 min: p = 1). In addition, low freezers' CORT level was
196 significantly higher at 60 min than high freezers (Tukey-Kramer test, p = 0.0039).

197 The total CORT response was quantified by the area-under-the-curve (AUC) of the
198 CORT response curve with the baseline CORT level (i.e. 0 min) being subtracted from
199 each time point. This quantification method took into account both the amplitude and
200 duration of the hormone response. Low freezers showed significantly higher total CORT
201 response than high freezers (t = 5.29, p = 0.031, Fig. 3b), as well as controls (t = 6.58, p
202 = 0.017, Fig. 3b). Furthermore, the total CORT response was significantly correlated with
203 freezing time across all fox urine exposed animals (R = 0.433, p = 0.035, n = 24, Fig. 3c),
204 and was also linked to long-lasting anxiety, evidenced by a significant correlation with the
205 EPM score measured 6 days after exposure across all animals tested (r = 0.36, p = 0.019,
206 n= 39, Fig. 3d). Taken together, these data demonstrate that low-freezing animals

207 displayed prolonged CORT response to predator scent stress, which was related to long-
208 term anxiety.

209

210 *Pre-trauma neural circuit functional connectivity predicted fear responses.*

211 In addition to behavioral tests, rsfMRI was performed before trauma exposure to
212 measure preexisting resting-state functional connectivity (RSFC) in neural circuits across
213 the whole brain. Echoing our behavioral data showing difference in freezing during the
214 very beginning of predator scent exposure, RSFC of multiple widespread neural circuits
215 significantly differed between high- and low-freezing animals (false discovery rate (FDR)
216 = 0.01, Supplement Fig. 4a). These regions/circuits have been implicated in stress
217 responses, processing of emotionally valent stimuli, olfactory function and freezing
218 behavior.

219 To identify the specific neural circuits correlated with the freezing phenotype, we
220 conducted a data-driven correlational analysis for all neural connections (67 regions
221 covering the whole brain, 2211 connections in total) between their RSFC and the
222 cumulative freezing time across all exposed animals (Fig. 4a, upper triangle). 15 neural
223 circuits exhibited a significant correlation between pre-exposure RSFC and freezing time
224 ($p < 0.05$, FDR corrected, Fig. 4a, lower triangle). Relative to high-freezing animals, six
225 of these connections showed stronger connectivity, whereas 9 showed lower connectivity
226 in low-freezing animals, suggesting that the pre-trauma connectivity within these circuits
227 might have predictive value for the freezing behavior during exposure. Fig. 4b showed
228 three representative RSFC maps, respectively generated with one region in these 15

229 connections as the seed (i.e. anterior cingulate cortex, AON and parabrachial nucleus).
230 Fig. 5 showed the correlational relationship between pre-trauma RSFC and freezing time
231 for all 15 circuits. The diagram of this freezing-associated network was summarized in
232 Fig. 6.

233 A closer examination of these 15 circuits revealed a comprehensive network
234 particularly involving the olfactory and stress-related brain areas. Specifically, low-
235 freezing animals showed stronger pre-trauma connectivity in two olfactory circuits (i.e.
236 AON-amygdala, and olfactory bulb-auditory cortex), two septal circuits (i.e. lateral septum
237 (LS)-bed nucleus of the stria terminalis (BNST), medial septum (MS)-prelimbic cortex
238 (PL)), and two circuits within the stress system (lateral hypothalamus-cortical amygdala
239 and lateral hypothalamus-amygdala). Stronger connectivity in the two olfactory circuits
240 suggest that odor may exert more influence on the amygdala and cortex in low-freezing
241 animals. Additionally, the LS-BNST projection might underlie stronger predator scent-
242 induced stress response in low-freezing animals. In support of this, both the LS and BNST
243 are activated by predator odor [24,25], and the BNST is actively involved in sustained fear
244 response to diffuse threat [26]. Stronger functional connectivity within the stress system can
245 also contribute to higher stress response and anxiety in low freezing animals.

246 Conversely, nine neural circuits showed weaker pre-trauma functional connectivity
247 in low-freezing animals, including two parabrachial nucleus (PBn) circuits (PBn-BNST and
248 PBn-hypothalamus), two nucleus accumbens (NAc) circuits (NAc-amygdala and NAc-
249 visual cortex), two zona inserta (ZI) circuits (ZI-pituitary gland and ZI-visceral cortex), as
250 well as the circuits of lateral olfactory tract nucleus (nLOT)-anterior cingulate cortex (ACC),
251 postsubiculum-agranular insula (AI), and globus pallidus (GP)-paraventricular (PVN)

252 hypothalamus. PBn is tightly related to olfactory function and electrophysiological data
253 show that calcitonin gene–related peptide (CGRP) in PBn has inhibitory effects in the
254 BNST [27]. Therefore, weaker connectivity in the PBn-BNST circuit suggests less inhibition
255 in BNST and could contribute to heightened anxiety in low freezing animals. Weaker
256 RSFC between the nLOT and ACC can reduce ACC's control over predator scent-
257 triggered defense reaction in low-freezing animals. In addition, the NAc-amygdala circuit
258 mediates avoidance behaviors [28], and decreased NAc connectivity was consistent with
259 report of the inverse association between NAc activity and the intensity of emotional
260 stress response [24], which might also be related to goal-directed motor behavior [29].
261 Furthermore, lower connectivity in ZI circuits (i.e. ZI-pituitary gland and ZI-visceral cortex)
262 may be involved in control of sympathetic visceral reactions and the hypothalamus–
263 pituitary–adrenal (HPA) axis activity [30]. Lastly, the GP-PVN hypothalamus projection,
264 known to involve corticotropin-releasing factor (CRF) neurons, were reported to link stress
265 response to motor output [31].

266 Taken together, these data indicate that differences in functional connectivity in
267 neural circuits particularly involving the olfactory and stress-related systems might
268 predispose animals to differential stress responses during predator scent exposure, which
269 can be linked to individual difference in subsequent development of PTSD-like behaviors
270 long after trauma exposure.

271

272 *Fear responses and long-term anxiety in fox-urine exposed animals were not due to the*
273 *novelty of the fox urine scent.*

To rule out the possibility that differential responses in fox-urine exposed animals resulted from the novelty component of the scent, we repeated the experiment with a lemon scent being used as the control scent in a separate cohort of animals (n=24). Lemon exposed animals showed virtually identical freezing (Supplement Fig. 5a, left, n = 6, two-sample t-test, t = 2.0, p = 0.16) and avoidance (distance from the pad, Supplement Fig. 5a**,** right, two-sample t-test, t = 1.14, p = 0.32) compared to animals exposed to no scent (i.e. air, n = 6), which ruled out the possibility that the novelty nature in the scent affected fear responses during exposure. In contrast, the fox urine exposed group (n = 12) maintained a greater mean distance from the cotton pad (one way ANOVA, $F_{(2,23)}$ = 11.61, p = 0.0004) than both air (p = 0.012) and lemon (p = 0.0006) exposed animals. In addition, fox urine exposed animals showed a trend of more freezing than non-traumatized animals (left, p = 0.056, lemon and air groups combined). Furthermore, consistent with the findings in the main cohort of animals, low-freezing animals exhibited stronger stress response during fox urine exposure and higher anxiety 6 days after exposure. Supplement Fig. 5b showed heat maps of the spatial distribution of time spent in the cage for the air-exposed, lemon-exposed, fox urine-exposed low freezing, and fox urine-exposed high freezing groups, respectively. The air and lemon groups showed no evident bias for either side of the cage, whereas the low-freezing group showed a strong bias toward the far end (from the pad) of the cage. High freezing rats also showed a bias toward the far end of the cage, but to a lesser extent. This result was also confirmed in the spatial distribution of the normalized freezing time for each group (supplement Fig. 5c), which displayed virtually no spatial bias in air and lemon groups, but leftward skewed distributions in high and low freezing rats, with an even stronger bias in low-freezing rats.

297 Supplement Fig. 5d showed the long-term anxiety measured using EPM performed 6
298 days post exposure in all four groups of animals. Low freezing animals showed a
299 significantly lower EPM score (one way ANOVA, $F_{(2,17)} = 4.2$, $p = 0.033$) compared to high
300 freezing animals ($p = 0.026$). Also consistent with our data in the main cohort of animals,
301 freezing time was positively correlated to the EPM score across all fox-urine exposed
302 animals ($r = 0.783$, $p = 0.0026$, Supplement Fig. 5e), but not in non-traumatized animals
303 ($r = 0.213$, $p = 0.506$, Supplement Fig. 5e). Taken together, these results ruled out the
304 possibility that differential short-term and long-term behavioral responses in fox-urine
305 exposed animals was due to the novel nature of the fox urine scent.

306

307 *Differential fear behavior during exposure and long-term anxiety between low- and high-*
308 *freezing animals were not caused by pre-exposure imaging.*

309 To rule out the possibility that differential fear response during predator scent
310 exposure and long-term anxiety between low- versus high-freezing animals indeed
311 resulted from predator scent exposure as oppose to other factors such as the acclimation
312 and/or imaging procedures, we also divided control animals into tertiles based on their
313 cumulative freezing time. No differences in avoidance behaviors including distance to the
314 cotton pad (two-sample t-test, $t = 1.22$, $p = 0.25$), the distribution of time spent in the cage
315 (two-way ANOVA, $F_{2,28} = 2.20$, $p = 0.13$, also see Supplement Fig. 6a), the distribution of
316 freezing time in the cage (repeated measures ANOVA, $F_{2,154} = 0.34$, $p = 0.98$), or long-
317 term anxiety level (EPM score, two-sample t-test, $t = 0.37$, $p = 0.72$) were observed
318 between low- and high-freezing control animals. In addition, unlike predator scent-
319 exposed animals, no neural connections exhibited correlation between pre-exposure

320 RSFC and freezing time, and no connection displayed significant RSFC difference
321 between low- and high-freezing control animals (Supplement Fig. 4b), indicating that
322 these animals showed virtually no difference in neural circuit function.

323 Furthermore, we repeated the fox urine exposure experiment in a separate cohort
324 of animals that were not previously acclimated or imaged (control, n = 20, fox urine
325 exposed, n = 35). Similar differential response during exposure was found in these
326 animals, with lower freezers generally exhibiting more avoidance from the fox urine
327 (Supplement Fig. 6b). These data suggest that the inherent difference between low and
328 high freezers was not caused by potential differential responsiveness to acclimation. This
329 result was supported by the data showing that all three groups of animals (i.e. low-freezing,
330 high-freezing and control) in the main cohort were acclimated to a similar degree,
331 reflected by their consistent motion levels during imaging (One-way ANOVA, $F_{(2,62)} = 1.23$,
332 $p = 0.3$, Supplement Fig.4c). These findings are also consistent with our previous
333 publications demonstrating that acclimation/imaging does not mask, nor does it interact
334 with the effect of predator stressor [21,23,32]. Taken together, these results confirmed that
335 differential fear behaviors and anxiety levels between low- and high-freezing animals
336 were not driven by the acclimation/imaging procedures as all control animals underwent
337 the identical procedures including imaging, except for being exposed to predator scent.

338

339 ## Discussion

340 Employing a longitudinal design, we investigated animals' individual variability in
341 stress response and subsequent development of PTSD-like behaviors following predator

342 scent exposure. We found that animals displayed large differences in freezing behavior
343 during fox urine exposure. Animals expressing less freezing exhibited increased
344 avoidance and tended to develop long-lasting heightened anxiety. Importantly, this
345 difference in behavioral responses was apparent at the beginning of predator scent
346 exposure, suggesting pre-existing vulnerability. This notion was supported by the rsfMRI
347 data showing significant pre-trauma difference in neural circuit connectivity between high-
348 and low-freezing animals. In addition, low-freezing animals showed a prolonged CORT
349 response to predator scent, which was correlated with freezing and long-lasting EPM
350 anxiety measurement. Taken together, this study provides important evidence supporting
351 the hypothesis that preexisting circuit function determines the defense response strategy
352 during threat and that this behavioral response might be directly related to the
353 development of PTSD. It also highlights the importance of studies that analyze factors
354 both before and after trauma for the study of PTSD.

355

356 *Freezing time alone might not be a reliable measure of response to threat.*

357 Behavioral response to stress is commonly categorized into fight, flight or freezing.
358 In rodent behavior testing, freezing is dominantly used as the measure of threat reaction.
359 Although freezing is a universal fear response, it manifests at intermediate levels of
360 predator threat [16]. Meanwhile, other types of threat-induced responses including fight-or-
361 flight, which is elicited during imminent threat [15], and avoidance can counteract the
362 measure of freezing. For this reason, the use of freezing as the only measure for stress
363 response of an individual animal can be problematic if alternative coping strategies are

364 not considered [33]. Indeed, there is growing evidence suggesting the ambiguity of freezing
365 time as it relates to stress [15,34].

366 In line with this concept, our data show that animals with the lowest freezing time
367 are in fact the most stressed subgroup. Their highly biased distribution in the total time
368 and freezing time at different distance to the cotton pad indicate that low-freezing animals
369 might have perceived a higher threat level and used strategies other than freezing (e.g.
370 avoidance), particularly at closer proximity to the pad. This result was corroborated by
371 significantly higher total CORT response during exposure in low-freezing animals, relative
372 to both high-freezing and control animals. This higher perceived threat level is likely a
373 crucial factor in maladaptation to stress response (e.g. higher long-lasting anxiety level),
374 which is in line with the literature investigating the role of threat perception in human PTSD
375 diagnoses [35]. Taken together, these results demonstrate that freezing time alone might
376 not be a reliable measure of reaction to threat. These data also highlight the importance
377 of separating subpopulations, in particular in stress studies, as key information can be
378 lost through the averaging of subpopulations that display bidirectional responses.

379 It has to be noted that lower freezing behavior in low freezers did not reflect a
380 reduced ability to respond to the predator scent. Low-freezing animals exhibited more
381 locomotor activity, measured by distance travelled during exposure (Supplemental Fig. 1,
382 One-way ANOVA, $F_{(2,62)} = 8.43$, $p = 0.001$, high freezers vs low-freezers, $p = 0.001$), and
383 more active avoidance from the fox urine. Furthermore, during exposure there was no
384 difference in mobility among low-, high-freezing and control groups, reflected by the
385 maximal speed (Supplement Fig. 1), also suggesting that low freezers were not
386 suppressed in their response to the fox scent. Different responses during exposure were

387 also not originated from any systematic bias in these measures among animals, because
388 during the habituation period prior to exposure, the three groups showed no difference in
389 freezing time (Supplement Fig. 2) or location distribution. Thus, the difference in freezing
390 to the predator scent likely reflects a difference in the defensive strategy selected.

391

392 *Behavioral and neuroendocrine reactions to a threat predict susceptibility to long-term*
393 *maladaptation*

394 Whether defensive reactions predict long-term emotion regulation and/or symptom
395 development has been an unresolved issue, largely due to lack of longitudinal studies
396 that follow up the relationship between behavioral reactions during trauma exposure and
397 the development of psychopathology [15]. Our longitudinal study demonstrates that freezing
398 during trauma exposure predicts long-term maladaptation in animals, supporting that
399 specific behavioral responses to a threat might predict susceptibility to long-term PTSD-
400 like behaviors.

401 The relationship between the behavioral reaction during stress and vulnerability to
402 stress maladaptation is corroborated by neuroendocrine measures during and following
403 predator scent stress. We observed that in low-freezing (i.e. vulnerable) animals, the
404 CORT response was prolonged and had a delayed return back to baseline after stress,
405 and this pattern of CORT response has been suggested as a marker of maladaptation to
406 stress in PTSD [36,37]. Correspondingly, in our study, both freezing time and the total CORT
407 response were correlated with the long-term anxiety measure. These data are also
408 consistent with the theory that stress hormone production is an important and protective

409 part of acute stress response triggering negative feedback on CORT production [38,39,41,42].
410 In fact, it has been shown that supplementing CORT at the time of trauma [44], or
411 immediately after trauma [45] has protective effects against PTSD symptom development
412 [38]. Taken together, our data indicate that individual variation in behavioral and hormonal
413 responses to stress can be key predictors of the development of emotion regulation and
414 chronic pathological states.

415

416 *Pre-trauma neural circuit function predisposes animals to differential stress response.*

417 *i) Connections between the olfactory and stress systems*

418 Our rsfMRI data suggest that sensory inputs play an important role in the stress
419 response and subsequent development of PTSD-like behaviors. AON has been shown
420 to be activated by variable stressors [46] including predator scent [47]. The mitral/tufted (MT)
421 cells in the olfactory bulb send their processes to AON [48], which projects to amygdala [49].
422 This connectivity suggests that the flow of olfactory information through the AON to the
423 amygdala could drive the stress response to predator scent. Stronger AON-amygdala
424 connectivity in low-freezing animals suggest that the olfactory cue could have a stronger
425 impact on amygdala activity, which would lead to stronger stress response. Conversely,
426 weaker nLOT-ACC connectivity in low-freezing animals indicates less ACC control during
427 predator scent exposure, which could affect the switching between freezing and active
428 defense modes [50]. These data also agree with the report that the olfactory cortex and its
429 connections with the stress system are tightly linked to stress hormone responses to
430 predator scent in rodents [51]. Taken together, these results highlight the importance of

431 sensory input in the stress response during predator scent exposure, which also suggest
432 that weaker sensory drive in the stress system may help promote resilience to trauma.

433 In addition to stronger sensory-stress connectivity, stronger functional connectivity
434 within the stress system was observed in low-freezing animals, consistent with their
435 higher stress response and anxiety. In particular, it is known that threat-induced
436 autonomic sympathetic responses are mediated by amygdala projections to the lateral
437 hypothalamus [15]. Stronger connectivity in this circuit could result in higher arousal, higher
438 cardiovascular activity and increased muscle tone during predator odor exposure in low-
439 freezing animals [52].

440 *ii) BNST circuits*

441 Our data also suggest that BNST may be involved in the neural network associated
442 with differential stress response during predator scent exposure. BNST, as a part of the
443 extended amygdala, is well known to be involved in sustained anxiety when a threat is
444 diffuse and/or uncertain [26,53] such as predator odor [25]. As a result, this region is particularly
445 associated with anxiety [54-56]. The anatomical connections between BNST and LS and
446 PBn have been well documented [27,57,58], but the specific function of these projections is
447 less well studied. It has been shown that CGRP in the PBn inhibits neurons of the BNST
448 [27], and BNST projections to the PBn dampen anxiety response [59]. These data support the
449 idea that a weaker PBn-BNST connection in low-freezing (i.e. vulnerable) animals caused
450 disinhibition of BNST activity, which led to a stronger stress response and heightened
451 long-lasting anxiety. Conversely, LS mediated activity, possibly again driven by olfactory
452 inputs [24], can potentiate BNST activity in these animals, and generate stronger stress
453 responses and heightened anxiety.

454 *iii) The hypothalamus-GP circuit*

455 Another interesting circuit that is coupled to freezing behavior is the PVN-GP
456 connection. CRF neurons in the PVN hypothalamus, amygdala and BNST send synapses
457 to the external GP [31], which expresses high levels of the primary CRF receptor (i.e.
458 CRFR1). These connections makes GP an entry point connecting the stress system with
459 the basal ganglia, which links the stress-relevant information to the directed movement [31].
460 Consistent with this notion, our data suggest that the pre-trauma connectivity in this circuit
461 is directly associated with stress-related behaviors in animals.

462 *iv) Possible contributions of other neural circuits to variable freezing behavior*

463 Stronger connectivity between the MS and PL can be linked to stronger fear in low-
464 freezing animals, given that PL promotes fear expression and avoidance [60,61]. Also
465 considering septal neurons are known to mediate the generation of theta oscillations [62,63],
466 the MS-PL connection may contribute to fear-associated theta rhythm in prefronto-
467 amygdalo-hippocampal pathways [64]. In addition, the postsubiculum-insula circuit
468 connectivity could be responsible for differential spatial movement in separate subgroups
469 of animals.

470 Lastly, a number of additional connections showed significant difference in pre-
471 trauma RSFC between low-freezing and high-freezing animals, even though their RSFC
472 was not correlated with freezing time. For example, lower RSFC between CA3 and
473 reticular nucleus (RT) was observed in low-freezing rats. RT is the hub connecting
474 hippocampus with PFC, and reduced connectivity in vulnerable rats might be due to less
475 prefrontal control of hippocampus [65]. Although premature, these results suggest that

476 preexisting neural circuit differences in vulnerable animals might reflect a sophisticated
477 network, and PTSD should be viewed as a network phenomenon.

478

479 *Relevance to human PTSD*

480 Our neural circuitry and neuroendocrine findings in animals echo PTSD research
481 in humans. Altered sensory function has also been reported in PTSD patients [66]. In
482 addition, a significant number of brain regions identified here (e.g. BNST, PFC) are tightly
483 related to anxiety disorders in humans [67], although the present study goes beyond static
484 neuroanatomy of individual brain regions and focuses on pre-existing neural circuit
485 function. Furthermore, human data also suggest that a dysregulated CORT response is
486 a predictor of vulnerability to subsequent development of PTSD [41,42,45,68]. Taken together,
487 these results provide compelling evidence supporting the relevance of the present study
488 to human PTSD.

489 In summary, our data demonstrate that differences in neural circuit function
490 present before trauma exposure may predispose animals to specific stress responses
491 and long-term PTSD-like behaviors. Future studies that focus on the causal relationship
492 between the baseline neural circuit function and behavioral responses during trauma
493 exposure and long-term outcome in PTSD-like behaviors will be needed to understand
494 pathological susceptibility to PTSD. For instance, it will be of particular interest to test
495 whether optogenetic manipulation of specific pathways based on the rsfMRI data during
496 trauma exposure can alter stress response and development of long-term PTSD-like
497 behaviors in animals.

498

499 ## Methods

500 Adult male LE rats (250-350g) were obtained from Charles River Laboratories
501 (Raleigh, North Carolina site). Rats were housed in pairs in Plexiglas cages with
502 controlled ambient temperature (22-24 °C) on a 12/12 hour day-dark schedule. Food and
503 water were provided ad libitum. A total of 87 rats were used in the present study, in which
504 23 rats were controls and 64 rats were exposed to predator scent using a single-episode
505 predator scent exposure in an inescapable environment paradigm. Two rats were
506 removed from the exposed group before analysis due to health concerns. All rats were
507 used for behavior tests and rsfMRI experiments. All animal procedures were reviewed
508 and approved by the Institutional Animal Care and Use Committee (IACUC) of the
509 Pennsylvania State University. The experimental procedure was summarized in Fig. 1a.

510 **Single-episode predator scent exposure**

511 Rats were exposed to a single episode of predator scent stress in an inescapable
512 environment for 10 min. The day prior to exposure, each rat was assigned to its own
513 exposure cage (i.e. a Plexiglas cage with no bedding) and habituated to the cage
514 environment for 30 min. The cage was left soiled after habituation. On the exposure day,
515 the rat was placed in its corresponding cage for a total of 12 min. After 2 min of adaptation,
516 a cotton pad sprayed with red fox urine was placed at the right end of the cage for another
517 10 mins (Red fox urine, Wild Life Research Center). The pad was put on a wire mesh
518 inside the cage, right below the lid and out of reach of the rat. The control animal was
519 exposed to the same cotton pad without fox urine. During exposure, the rat was recorded

520 by a video camera. Following predator scent exposure, the rat was returned to his home
521 cage and left undisturbed for 6 days.

522 **Elevated plus maze (EPM)**

523 The EPM test was performed to measure the anxiety level 6 days after trauma
524 exposure. The maze consisted of four perpendicular arms forming a cross and elevated
525 50 cm from the floor. Two arms were closed, opposed to each other and enclosed by 40-
526 cm high walls. The remaining two arms, also opposed to each other, were completely
527 open. A camera was placed directly above the maze to record the rat movement.

528 To perform the test, the rat was initially placed in the center of the maze facing one
529 open arm and allowed to freely explore the maze for 5 min. The times spent in the open
530 and closed arms were determined. The ratio of time in open arms versus that in both open
531 and closed arms [i.e. open/(open+closed)] was calculated to provide a measure of anxiety
532 level. A lower score of this ratio indicates a higher level of anxiety. The maze was cleaned
533 with a 70% alcohol solution in water between tests.

534 **CORT Measurement**

535 Rats (n = 39) had blood samples collected to quantify the hormonal response to
536 stress. Corticosterone (CORT) level was measured immediately before predator scent
537 exposure (i.e. 0 min) and 30 min, 60 min, and 120 min after exposure to quantify the
538 dynamic response to predator scent stress exposure. Initial blood samples were collected
539 through tail nick, with subsequent time point samples collected by disturbing the tail scab.
540 Samples were collected using heparin coated microtubes with capillary tube inserts (RAM
541 Scientific Safe-T-Fill, Nashville, TN, USA). Samples were centrifuged to obtain plasma

542 and stored at -20 ºC. The plasma CORT level was then quantified using CORT enzyme-
543 linked immunosorbent assay (ELISA) kit (Enzo life sciences Inc. Ann Arbor, MI. Cat ADI-
544 901-097) according to the manufacturer's manual. The total CORT response for each
545 animal was quantified by the area-under-the-curve of the CORT response curve,
546 calculated by the summation of the CORT amplitude across all time points with the CORT
547 level at 0 min (i.e. baseline) being subtracted at each time point. This measurement took
548 into account both the amplitude and duration of the CORT response and represented the
549 total output of the hypothalamus-pituitary-adrenal axis.

550 **Acclimation and rsfMRI data acquisition**

551 All rats were scanned before the trauma exposure experiment. Before imaging,
552 animals were acclimated to a 'mock' imaging environment for 7 days. This acclimation
553 protocol was employed to diminish the stress and motion of the subject during scans [69].
554 The rat was first briefly anesthetized with 2-4% isoflurane in oxygen (3-5 min). The head
555 was restrained with a bite bar, nose bar and side pads that restricted the head motion. A
556 pair of shoulder bars and a body tube maintained the body in place without impeding
557 ventilation. Animals were allowed to regain consciousness by discontinuing isoflurane
558 after being set up in the restrainer, typically in 10 mins. The rat was then placed in a dark
559 ventilated box and the sound of different MRI sequences was played, presenting an
560 environment mimicking MRI scanning. All rats were given 7 daily acclimation sessions
561 with a gradually increasing acclimation period (15, 30, 45, 60, 60, 60 and 60 min from day
562 1 to day 7). A similar approach has also been applied by other research groups [70-72].

563 At least 2 days after acclimation, MRI scans were performed in a 7-Tesla scanner
564 interfaced with the Bruker console system (Bruker, Germany). The rat was first briefly

565 anesthetized with 2-4% isoflurane in oxygen and set up in the same restrainer with a built-
566 in birdcage 1H radiofrequency volume coil. Anesthesia was then discontinued, and the
567 rat was allowed to regain consciousness and placed into the MRI magnet bore. rsfMRI
568 data were obtained using a single shot gradient-echo echo-planar imaging sequence with
569 the parameters of repetition time (TR) = 1 sec, echo time (TE) = 13.8 ms, 64 × 64 matrix
570 size, 20 slices with 1 mm thickness, field of view (FOV) = 32 × 32 mm^2, in-plane resolution
571 = 500 × 500 μm^2. Each rat was scanned for 2400 EPI volumes per scan session.
572 Anatomical images were also acquired using a fast spin-echo sequence with the
573 parameters of TR = 1500 ms; TE = 8 ms; matrix size = 256 × 256; FOV = 3.2 × 3.2 cm^2;
574 slice number = 20; slice thickness = 1 mm; RARE factor = 8.

575 **rsfMRI data processing**

576 rsfMRI images were preprocessed by performing alignment using Medical Image
577 Visualization and Analysis (MIVA, http://ccni.wpi.edu/), motion correction using SPM 12
578 (http://www.fil.ion.ucl.ac.uk/spm/), spatial smoothing (Gaussian kernel: FWHM = 0.75 mm)
579 and temporal smoothing (band-pass filter, cutoff frequencies: 0.01-0.1Hz), and regression
580 of motion parameters and signals from the white matter and ventricles as described in
581 past studies [20,22,23,73]. Before performing these steps, EPI volumes with relative framewise
582 displacement (FD) > 0.2 mm and their immediate temporal neighbors were first removed
583 [74]. In addition, the first 10 volumes of each rsfMRI run were also removed to ensure the
584 magnetization was at steady state.

585 Functional connectivity analysis was conducted using region-of-interest (ROI)
586 based correlational analysis. This method evaluated the RSFC by quantifying the
587 Pearson correlation coefficient of regionally averaged spontaneous BOLD signals

588 between different brain regions. Seed maps were generated by correlating the regionally
589 averaged seed time course with the time course of each brain voxel. A linear mixed effect
590 model was used to determine the overall effect on RSFC of each group of rats, while
591 removing any random effect from different batches of animals.

592

593 **References:**

594 1 Charney, D. S. Psychobiological mechanisms of resilience and vulnerability:
595 implications for successful adaptation to extreme stress. *Am J Psychiatry* **161**, 195-
596 216, doi:10.1176/appi.ajp.161.2.195 (2004).
597 2 Yehuda, R. & LeDoux, J. Response variation following trauma: a translational
598 neuroscience approach to understanding PTSD. *Neuron* **56**, 19-32,
599 doi:10.1016/j.neuron.2007.09.006 (2007).
600 3 Feder, A., Nestler, E. J. & Charney, D. S. Psychobiology and molecular genetics
601 of resilience. *Nat Rev Neurosci* **10**, 446-457, doi:10.1038/nrn2649 (2009).
602 4 Gilbertson, M. W. *et al.* Smaller hippocampal volume predicts pathologic
603 vulnerability to psychological trauma. *Nat Neurosci* **5**, 1242-1247,
604 doi:10.1038/nn958 (2002).
605 5 Bonne, O. *et al.* Longitudinal MRI study of hippocampal volume in trauma survivors
606 with PTSD. *Am J Psychiatry* **158**, 1248-1251, doi:10.1176/appi.ajp.158.8.1248
607 (2001).
608 6 McEwen, B. S., Nasca, C. & Gray, J. D. Stress Effects on Neuronal Structure:
609 Hippocampus, Amygdala, and Prefrontal Cortex. *Neuropsychopharmacology* **41**,
610 3-23, doi:10.1038/npp.2015.171 (2016).
611 7 Logue, M. W. *et al.* Smaller Hippocampal Volume in Posttraumatic Stress Disorder:
612 A Multisite ENIGMA-PGC Study: Subcortical Volumetry Results From
613 Posttraumatic Stress Disorder Consortia. *Biol Psychiatry* **83**, 244-253,
614 doi:10.1016/j.biopsych.2017.09.006 (2018).

615 8 Yehuda, R. Advances in understanding neuroendocrine alterations in PTSD and
616 their therapeutic implications. *Ann N Y Acad Sci* **1071**, 137-166,
617 doi:10.1196/annals.1364.012 (2006).
618 9 Milad, M. R. *et al.* Neurobiological basis of failure to recall extinction memory in
619 posttraumatic stress disorder. *Biol Psychiatry* **66**, 1075-1082,
620 doi:10.1016/j.biopsych.2009.06.026S0006-3223(09)00896-8 [pii] (2009).
621 10 Shin, L. M. *et al.* Exaggerated activation of dorsal anterior cingulate cortex during
622 cognitive interference: a monozygotic twin study of posttraumatic stress disorder.
623 *Am J Psychiatry* **168**, 979-985, doi:10.1176/appi.ajp.2011.09121812 (2011).
624 11 Goswami, S., Rodriguez-Sierra, O., Cascardi, M. & Pare, D. Animal models of
625 post-traumatic stress disorder: face validity. *Frontiers in neuroscience* **7**, 89,
626 doi:10.3389/fnins.2013.00089 (2013).
627 12 Deslauriers, J., Toth, M., Der-Avakian, A. & Risbrough, V. B. Current Status of
628 Animal Models of Posttraumatic Stress Disorder: Behavioral and Biological
629 Phenotypes, and Future Challenges in Improving Translation. *Biol Psychiatry* **83**,
630 895-907, doi:10.1016/j.biopsych.2017.11.019 (2018).
631 13 Flandreau, E. I. & Toth, M. Animal Models of PTSD: A Critical Review. *Current*
632 *topics in behavioral neurosciences*, doi:10.1007/7854_2016_65 (2017).
633 14 Cohen, H. & Zohar, J. An animal model of posttraumatic stress disorder: the use
634 of cut-off behavioral criteria. *Ann N Y Acad Sci* **1032**, 167-178 (2004).
635 15 Roelofs, K. Freeze for action: neurobiological mechanisms in animal and human
636 freezing. *Philos Trans R Soc Lond B Biol Sci* **372**, doi:10.1098/rstb.2016.0206
637 (2017).
638 16 Fanselow, M. S. Neural organization of the defensive behavior system responsible
639 for fear. *Psychon Bull Rev* **1**, 429-438, doi:10.3758/BF03210947 (1994).
640 17 Liang, Z., King, J. & Zhang, N. Uncovering intrinsic connectional architecture of
641 functional networks in awake rat brain. *J Neurosci* **31**, 3776-3783 (2011).
642 18 Liang, Z., King, J. & Zhang, N. Anticorrelated resting-state functional connectivity
643 in awake rat brain. *Neuroimage* **59**, 1190-1199, doi:S1053-8119(11)00896-2
644 [pii]10.1016/j.neuroimage.2011.08.009 (2012).

645 19 Ma, Z. *et al.* Functional atlas of the awake rat brain: A neuroimaging study of rat
646 brain specialization and integration. *Neuroimage* **170**, 95-112,
647 doi:10.1016/j.neuroimage.2016.07.007 (2018).
648 20 Ma, Z. & Zhang, N. Temporal transitions of spontaneous brain activity. *eLife* **7**,
649 doi:10.7554/eLife.33562 (2018).
650 21 Gao, Y. R. *et al.* Time to wake up: Studying neurovascular coupling and brain-wide
651 circuit function in the un-anesthetized animal. *Neuroimage*,
652 doi:10.1016/j.neuroimage.2016.11.069 (2016).
653 22 Liang, Z., King, J. & Zhang, N. Intrinsic organization of the anesthetized brain. *J*
654 *Neurosci* **32**, 10183-10191, doi:10.1523/JNEUROSCI.1020-12.2012 (2012).
655 23 Liang, Z., King, J. & Zhang, N. Neuroplasticity to a single-episode traumatic stress
656 revealed by resting-state fMRI in awake rats. *Neuroimage* **103**, 485-491,
657 doi:10.1016/j.neuroimage.2014.08.050 (2014).
658 24 Ubeda-Contreras, J., Marin-Blasco, I., Nadal, R. & Armario, A. Brain c-fos
659 expression patterns induced by emotional stressors differing in nature and intensity.
660 *Brain structure & function* **223**, 2213-2227, doi:10.1007/s00429-018-1624-2 (2018).
661 25 Janitzky, K., D'Hanis, W., Krober, A. & Schwegler, H. TMT predator odor activated
662 neural circuit in C57BL/6J mice indicates TMT-stress as a suitable model for
663 uncontrollable intense stress. *Brain Res* **1599**, 1-8,
664 doi:10.1016/j.brainres.2014.12.030 (2015).
665 26 Daldrup, T., Lesting, J., Meuth, P., Seidenbecher, T. & Pape, H. C. Neuronal
666 correlates of sustained fear in the anterolateral part of the bed nucleus of stria
667 terminalis. *Neurobiology of learning and memory* **131**, 137-146,
668 doi:10.1016/j.nlm.2016.03.020 (2016).
669 27 Gungor, N. Z. & Pare, D. CGRP inhibits neurons of the bed nucleus of the stria
670 terminalis: implications for the regulation of fear and anxiety. *J Neurosci* **34**, 60-65,
671 doi:10.1523/JNEUROSCI.3473-13.2014 (2014).
672 28 Ramirez, F., Moscarello, J. M., LeDoux, J. E. & Sears, R. M. Active avoidance
673 requires a serial basal amygdala to nucleus accumbens shell circuit. *J Neurosci*
674 **35**, 3470-3477, doi:10.1523/JNEUROSCI.1331-14.2015 (2015).

675 29 Da Cunha, C., Gomez, A. A. & Blaha, C. D. The role of the basal ganglia in
676 motivated behavior. *Rev Neurosci* **23**, 747-767, doi:10.1515/revneuro-2012-0063
677 (2012).
678 30 Mitrofanis, J. Some certainty for the "zone of uncertainty"? Exploring the function
679 of the zona incerta. *Neuroscience* **130**, 1-15,
680 doi:10.1016/j.neuroscience.2004.08.017 (2005).
681 31 Hunt, A. J., Jr. *et al.* Paraventricular hypothalamic and amygdalar CRF neurons
682 synapse in the external globus pallidus. *Brain structure & function* **223**, 2685-2698,
683 doi:10.1007/s00429-018-1652-y (2018).
684 32 Dopfel, D. & Zhang, N. Mapping stress networks using functional magnetic
685 resonance imaging in awake animals. *Neurobiol Stress* **9**, 251-263,
686 doi:10.1016/j.ynstr.2018.06.002 (2018).
687 33 Paré, D. & Quirk, G. J. When scientific paradigms lead to tunnel vision: lessons
688 from the study of fear. *npj Science of Learning* **2**, 6, doi:10.1038/s41539-017-0007-
689 4 (2017).
690 34 Gruene, T. M., Flick, K., Stefano, A., Shea, S. D. & Shansky, R. M. Sexually
691 divergent expression of active and passive conditioned fear responses in rats.
692 *eLife* **4**, doi:10.7554/eLife.11352 (2015).
693 35 Holbrook, T. L., Hoyt, D. B., Stein, M. B. & Sieber, W. J. Perceived threat to life
694 predicts posttraumatic stress disorder after major trauma: risk factors and
695 functional outcome. *J Trauma* **51**, 287-292; discussion 292-283 (2001).
696 36 Yehuda, R. Current status of cortisol findings in post-traumatic stress disorder.
697 *Psychiatr Clin North Am* **25**, 341-368, vii (2002).
698 37 Mouthaan, J. *et al.* The role of acute cortisol and DHEAS in predicting acute and
699 chronic PTSD symptoms. *Psychoneuroendocrinology* **45**, 179-186,
700 doi:10.1016/j.psyneuen.2014.04.001 (2014).
701 38 Rao, R. P., Anilkumar, S., McEwen, B. S. & Chattarji, S. Glucocorticoids protect
702 against the delayed behavioral and cellular effects of acute stress on the amygdala.
703 *Biol Psychiatry* **72**, 466-475, doi:10.1016/j.biopsych.2012.04.008 (2012).
704 39 McEwen, B. S. *et al.* Mechanisms of stress in the brain. *Nat Neurosci* **18**, 1353-
705 1363, doi:10.1038/nn.4086 (2015).

706 40 Whitaker, A. M. & Gilpin, N. W. Blunted hypothalamo-pituitary adrenal axis
707 response to predator odor predicts high stress reactivity. *Physiol Behav* **147**, 16-
708 22, doi:10.1016/j.physbeh.2015.03.033 (2015).
709 41 Yehuda, R., McFarlane, A. C. & Shalev, A. Y. Predicting the development of
710 posttraumatic stress disorder from the acute response to a traumatic event. *Biol*
711 *Psychiatry* **44**, 1305-1313 (1998).
712 42 Delahanty, D. L., Raimonde, A. J. & Spoonster, E. Initial posttraumatic urinary
713 cortisol levels predict subsequent PTSD symptoms in motor vehicle accident
714 victims. *Biol Psychiatry* **48**, 940-947 (2000).
715 43 Weaver, I. C. *et al.* Reversal of maternal programming of stress responses in adult
716 offspring through methyl supplementation: altering epigenetic marking later in life.
717 *J Neurosci* **25**, 11045-11054, doi:10.1523/JNEUROSCI.3652-05.2005 (2005).
718 44 Schelling, G. *et al.* Efficacy of hydrocortisone in preventing posttraumatic stress
719 disorder following critical illness and major surgery. *Ann N Y Acad Sci* **1071**, 46-
720 53, doi:10.1196/annals.1364.005 (2006).
721 45 Zohar, J. *et al.* High dose hydrocortisone immediately after trauma may alter the
722 trajectory of PTSD: interplay between clinical and animal studies. *European*
723 *neuropsychopharmacology : the journal of the European College of*
724 *Neuropsychopharmacology* **21**, 796-809, doi:10.1016/j.euroneuro.2011.06.001
725 (2011).
726 46 Cullinan, W. E., Herman, J. P., Battaglia, D. F., Akil, H. & Watson, S. J. Pattern
727 and time course of immediate early gene expression in rat brain following acute
728 stress. *Neuroscience* **64**, 477-505 (1995).
729 47 Dielenberg, R. A., Hunt, G. E. & McGregor, I. S. "When a rat smells a cat": the
730 distribution of Fos immunoreactivity in rat brain following exposure to a predatory
731 odor. *Neuroscience* **104**, 1085-1097 (2001).
732 48 Friedrich, R. W. Olfactory neuroscience: beyond the bulb. *Curr Biol* **21**, R438-440,
733 doi:10.1016/j.cub.2011.04.036 (2011).
734 49 Ferrer, N. G. Efferent projections of the anterior olfactory nucleus. *J Comp Neurol*
735 **137**, 309-320, doi:10.1002/cne.901370305 (1969).

736 50 Gozzi, A. *et al.* A neural switch for active and passive fear. *Neuron* **67**, 656-666,
737 doi:10.1016/j.neuron.2010.07.008 (2010).
738 51 Kondoh, K. *et al.* A specific area of olfactory cortex involved in stress hormone
739 responses to predator odours. *Nature* **532**, 103-106, doi:10.1038/nature17156
740 (2016).
741 52 Keay, K. A. & Bandler, R. Parallel circuits mediating distinct emotional coping
742 reactions to different types of stress. *Neurosci Biobehav Rev* **25**, 669-678 (2001).
743 53 Walker, D. L. & Davis, M. Role of the extended amygdala in short-duration versus
744 sustained fear: a tribute to Dr. Lennart Heimer. *Brain structure & function* **213**, 29-
745 42, doi:10.1007/s00429-008-0183-3 (2008).
746 54 Somerville, L. H., Whalen, P. J. & Kelley, W. M. Human bed nucleus of the stria
747 terminalis indexes hypervigilant threat monitoring. *Biol Psychiatry* **68**, 416-424,
748 doi:10.1016/j.biopsych.2010.04.002 (2010).
749 55 Grupe, D. W. & Nitschke, J. B. Uncertainty and anticipation in anxiety: an
750 integrated neurobiological and psychological perspective. *Nat Rev Neurosci* **14**,
751 488-501, doi:10.1038/nrn3524 (2013).
752 56 Davis, M. Neural systems involved in fear and anxiety measured with fear-
753 potentiated startle. *Am Psychol* **61**, 741-756, doi:10.1037/0003-066X.61.8.741
754 (2006).
755 57 Dong, H. W. & Swanson, L. W. Projections from bed nuclei of the stria terminalis,
756 posterior division: implications for cerebral hemisphere regulation of defensive and
757 reproductive behaviors. *J Comp Neurol* **471**, 396-433, doi:10.1002/cne.20002
758 (2004).
759 58 Dong, H. W. & Swanson, L. W. Organization of axonal projections from the
760 anterolateral area of the bed nuclei of the stria terminalis. *J Comp Neurol* **468**, 277-
761 298, doi:10.1002/cne.10949 (2004).
762 59 Tovote, P., Fadok, J. P. & Luthi, A. Neuronal circuits for fear and anxiety. *Nat Rev*
763 *Neurosci* **16**, 317-331, doi:10.1038/nrn3945 (2015).
764 60 Sierra-Mercado, D., Padilla-Coreano, N. & Quirk, G. J. Dissociable roles of
765 prelimbic and infralimbic cortices, ventral hippocampus, and basolateral amygdala

766 in the expression and extinction of conditioned fear. *Neuropsychopharmacology*
767 **36**, 529-538, doi:10.1038/npp.2010.184 (2011).
768 61 Diehl, M. M. *et al.* Active avoidance requires inhibitory signaling in the rodent
769 prelimbic prefrontal cortex. *eLife* **7**, doi:10.7554/eLife.34657 (2018).
770 62 Vertes, R. P. & Kocsis, B. Brainstem-diencephalo-septohippocampal systems
771 controlling the theta rhythm of the hippocampus. *Neuroscience* **81**, 893-926 (1997).
772 63 Buzsaki, G. Theta oscillations in the hippocampus. *Neuron* **33**, 325-340 (2002).
773 64 Lesting, J. *et al.* Directional theta coherence in prefrontal cortical to amygdalo-
774 hippocampal pathways signals fear extinction. *PLoS One* **8**, e77707,
775 doi:10.1371/journal.pone.0077707 (2013).
776 65 Marek, R. *et al.* Hippocampus-driven feed-forward inhibition of the prefrontal cortex
777 mediates relapse of extinguished fear. *Nat Neurosci* **21**, 384-392,
778 doi:10.1038/s41593-018-0073-9 (2018).
779 66 Zhang, J. *et al.* Decreased gray matter volume in the left hippocampus and bilateral
780 calcarine cortex in coal mine flood disaster survivors with recent onset PTSD.
781 *Psychiatry Res* **192**, 84-90, doi:10.1016/j.pscychresns.2010.09.001 (2011).
782 67 Lebow, M. A. & Chen, A. Overshadowed by the amygdala: the bed nucleus of the
783 stria terminalis emerges as key to psychiatric disorders. *Molecular psychiatry* **21**,
784 450-463, doi:10.1038/mp.2016.1 (2016).
785 68 Schelling, G., Roozendaal, B. & De Quervain, D. J. Can posttraumatic stress
786 disorder be prevented with glucocorticoids? *Ann N Y Acad Sci* **1032**, 158-166,
787 doi:10.1196/annals.1314.013 (2004).
788 69 King, J. A. *et al.* Procedure for minimizing stress for fMRI studies in conscious rats.
789 *J Neurosci Methods* **148**, 154-160 (2005).
790 70 Bergmann, E., Zur, G., Bershadsky, G. & Kahn, I. The Organization of Mouse and
791 Human Cortico-Hippocampal Networks Estimated by Intrinsic Functional
792 Connectivity. *Cereb Cortex* **26**, 4497-4512, doi:10.1093/cercor/bhw327 (2016).
793 71 Yoshida, K. *et al.* Physiological effects of a habituation procedure for functional
794 MRI in awake mice using a cryogenic radiofrequency probe. *J Neurosci Methods*
795 **274**, 38-48, doi:10.1016/j.jneumeth.2016.09.013 (2016).

796 72 Chang, P. C. *et al.* Novel method for functional brain imaging in awake minimally
797 restrained rats. *J Neurophysiol* **116**, 61-80, doi:10.1152/jn.01078.2015 (2016).
798 73 Liang, Z., Liu, X. & Zhang, N. Dynamic resting state functional connectivity in
799 awake and anesthetized rodents. *Neuroimage* **104**, 89-99,
800 doi:10.1016/j.neuroimage.2014.10.013 (2015).
801 74 Power, J. D., Barnes, K. A., Snyder, A. Z., Schlaggar, B. L. & Petersen, S. E.
802 Spurious but systematic correlations in functional connectivity MRI networks arise
803 from subject motion. *Neuroimage* **59**, 2142-2154,
804 doi:10.1016/j.neuroimage.2011.10.018 (2012).

805

806

807

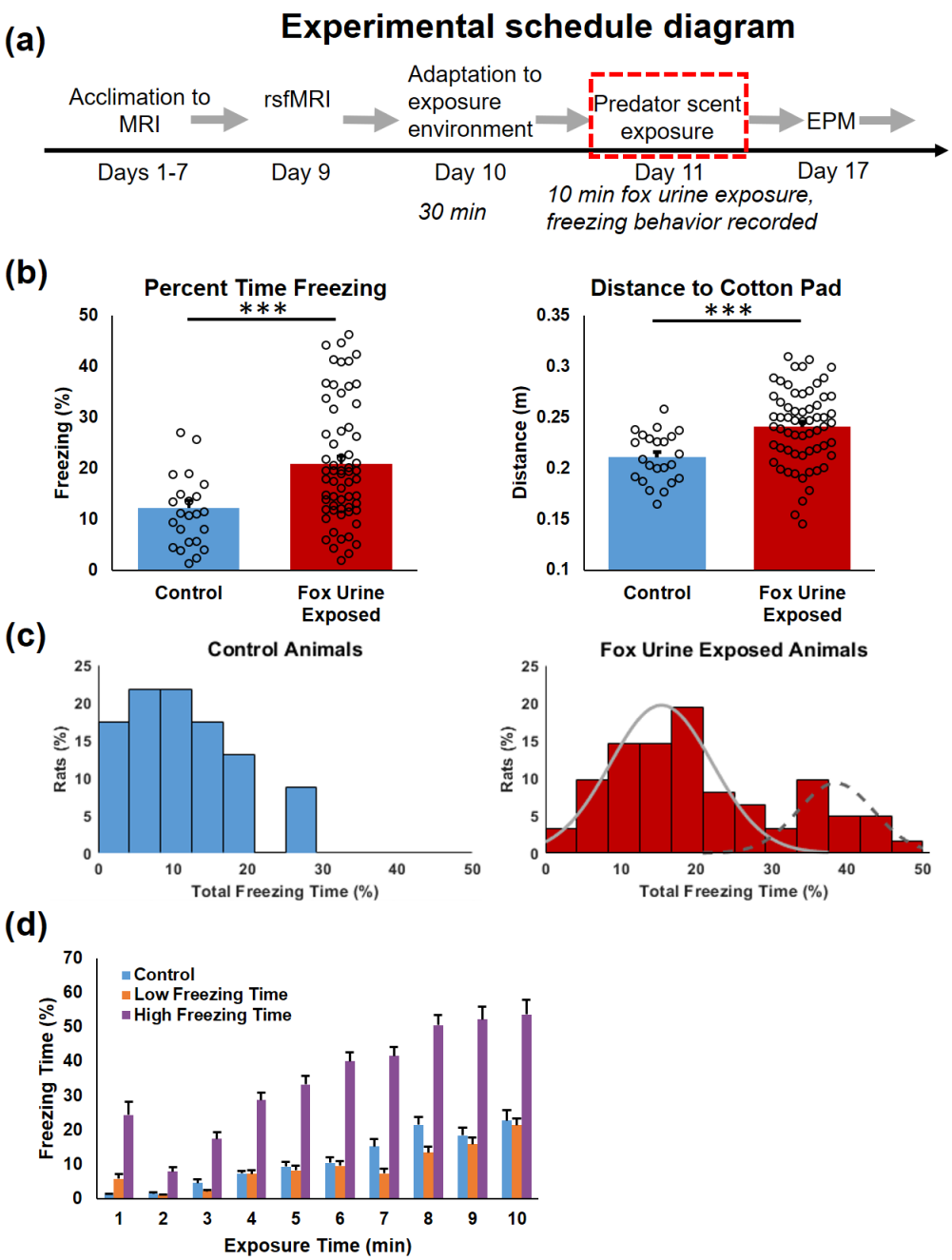

Figure 1. Freezing time during the 10-min exposure session in control (n = 23) and fox urine exposed (n = 62) groups. **a**) Diagram of experimental schedule. **b**) Fox urine exposed animals showed a significantly longer freezing time (left, $p < 0.0005$, in percentage) and greater mean distance (right, $p < 0.0007$, in meters) from the cotton pad than controls. **c**) The distributions of individual animals' freezing time in the control group (left) and the exposed group (right) displayed as probability histograms. The freezing time distribution in exposed animals was fit to a Gaussian mixture model which demonstrated a bimodal distribution. **d**) Freezing time each min plotted as a function of time in low-freezing (n=21), high-freezing (n=21) and control animals during fox urine exposure. The high freezing animals displayed higher freezing phenotype during the first minute of

819 exposure, with a significantly longer freezing time than both low freezing and control
820 animals from the 1st minute through the 10th minute ($p < 0.005$ for each minute of
821 exposure).

822

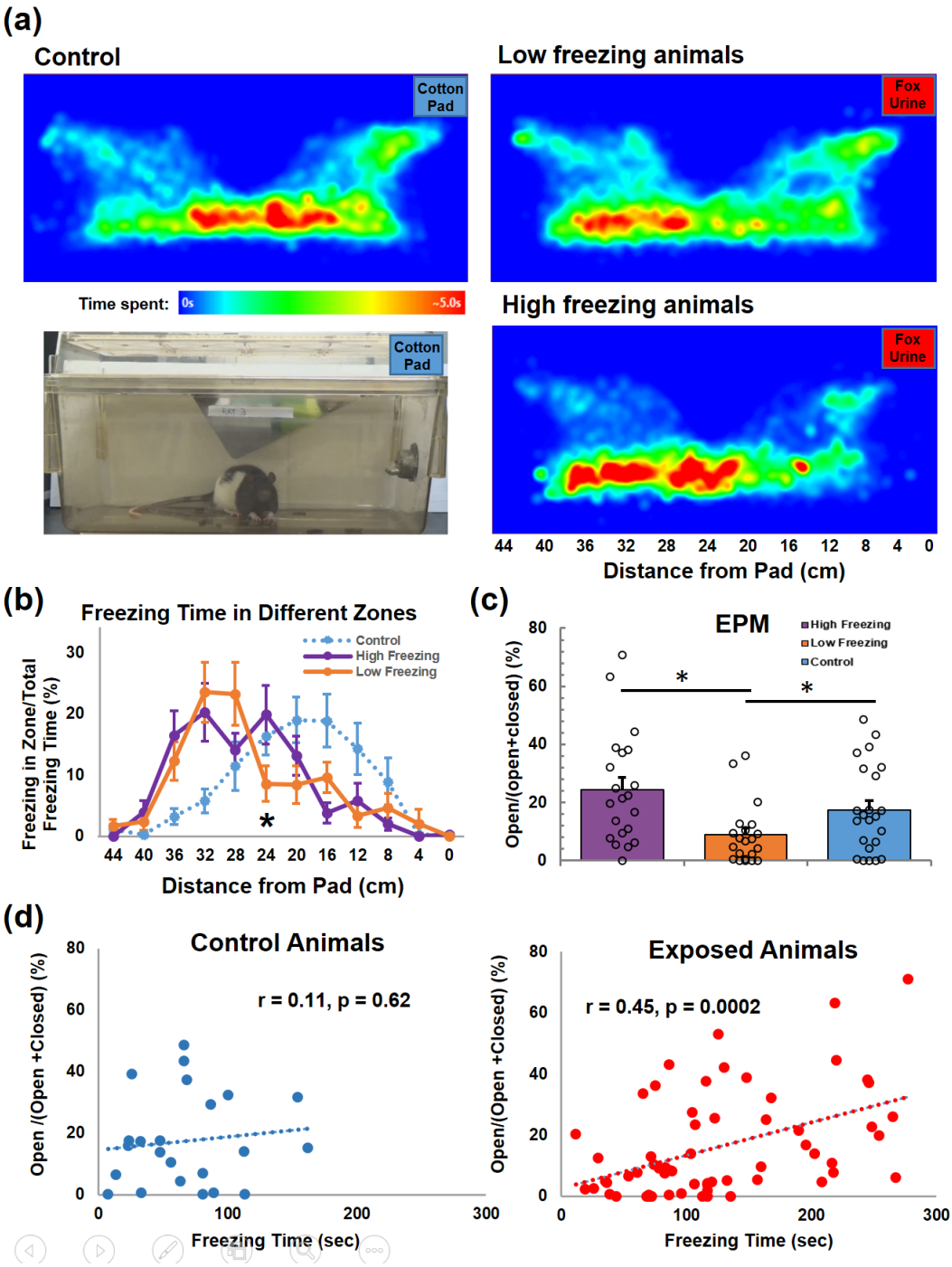

Figure 2. Low-freezing animals exhibited stronger stress response during fox urine exposure and higher anxiety 6 days after exposure. **a**) Heat maps of the total time at each location for the control, low freezing, and high freezing groups. The control group showed no evident bias for either side of the cage. The low freezing group showed a strong bias toward the far end (from the pad) of the cage, while the high freezing rats also showed a bias toward the far end of the cage, but to a lesser extent. **b**) The distribution of the percent freezing time for each group across the cage, divided into 12 equivalent-sized zones. The x-axis indicates the distance to the pad from the center of each zone. Similar to the

distributions of total time spent, the percent freezing time in control rats displayed little bias for either side of the cage. High and low freezing animals showed a bias of percent freezing time toward the far end of the cage, with the low-freezing rats showing even stronger bias than high-freezing animals, evidenced by significantly lower percent freezing time of the low-freezing group in the zone 24 cm away from the pad compared to the high-freezing group ($p = 0.026$). **c**) Elevated plus maze performed 6 days post exposure in all three groups of animals. Low-freezing animals showed a significantly lower EPM score (open/open+closed arm time) compared to both control ($p = 0.030$) and high-freezing animals ($p = 0.0017$), while no significant difference was seen between control and high freezing groups. **d**) The freezing time was positively correlated to the EPM score across all exposed animals ($r = 0.45$, $p = 0.0002$), but not across control animals ($r = 0.11$, $p = 0.62$).

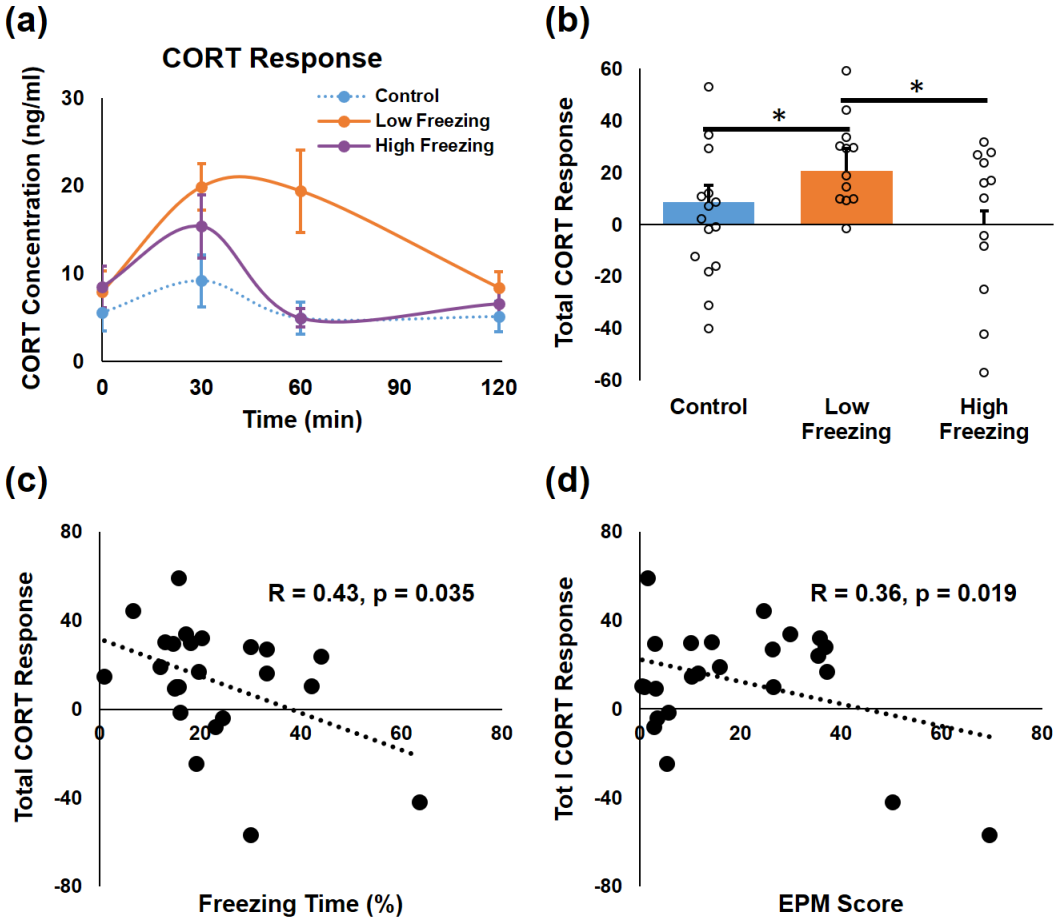

Figure 3. Corticosterone (CORT) response to fox urine exposure. **a**) The time course of CORT (in ng/ml) for high-, low-freezing and control animals. There was a significant difference in CORT level changes over time among three groups (Two-way repeated ANOVA, $F_{group \times time}$ (6,108) = 2.84, p = 0.023). Control animals showed no appreciable CORT change across time (One-way repeated ANOVA, F_{time} (3,56) = 0.8, p = 0.50). High-freezing animals exhibited a relatively short CORT response, peaking at 30 min and returning to baseline at 60 min (Tukey-Kramer test, 30 min vs 60 min: p = 0.049; 0 min vs 60 min: p = 0.54; 60 min vs 120 min: p = 0.93). The peak amplitude of CORT response at 30 min was comparable between high- and low-freezing animals (Tukey-Kramer test, p = 0.59). However, relative to high-freezing rats, the CORT response in low-freezing animals was prolonged, maintained at a high level at 60 min (Tukey-Kramer test, 30 min vs 60 min: p = 1; 0 min vs 60 min: p = 0.0005) and had a delayed return to baseline at 120 min (Tukey-Kramer test, 60 min vs 120 min: p = 0.0098; 0 min vs 120 min: p = 1). In addition, low freezers' CORT level was significantly higher at 60 min than high freezers (Tukey-Kramer test, p = 0.0039). **b**) Total CORT response was quantified by the area-under-the-curve (AUC) of the CORT response curve, with the baseline CORT level (i.e. 0 min) being subtracted from each time point. This quantification method takes into account both the amplitude and length of the hormone response and represents the total output of the hypothalamus-pituitary-adrenal axis during exposure. Low-freezing animals showed a significant higher total CORT response than high-freezing (p = 0.031) and control (p = 0.017) animals. **c**) Significant correlation between the total CORT responsive

867 (y-axis) and freezing time during exposure across all fox urine exposed animals ($r = 0.43$,
868 $p = 0.035$). **d**) Significant correlation ($r = 0.36$, $p = 0.019$) between the total CORT
869 response (y-axis) and EPM score (open/open+closed arm time, x-axis) measured 6 days
870 post exposure across all animals tested.

871

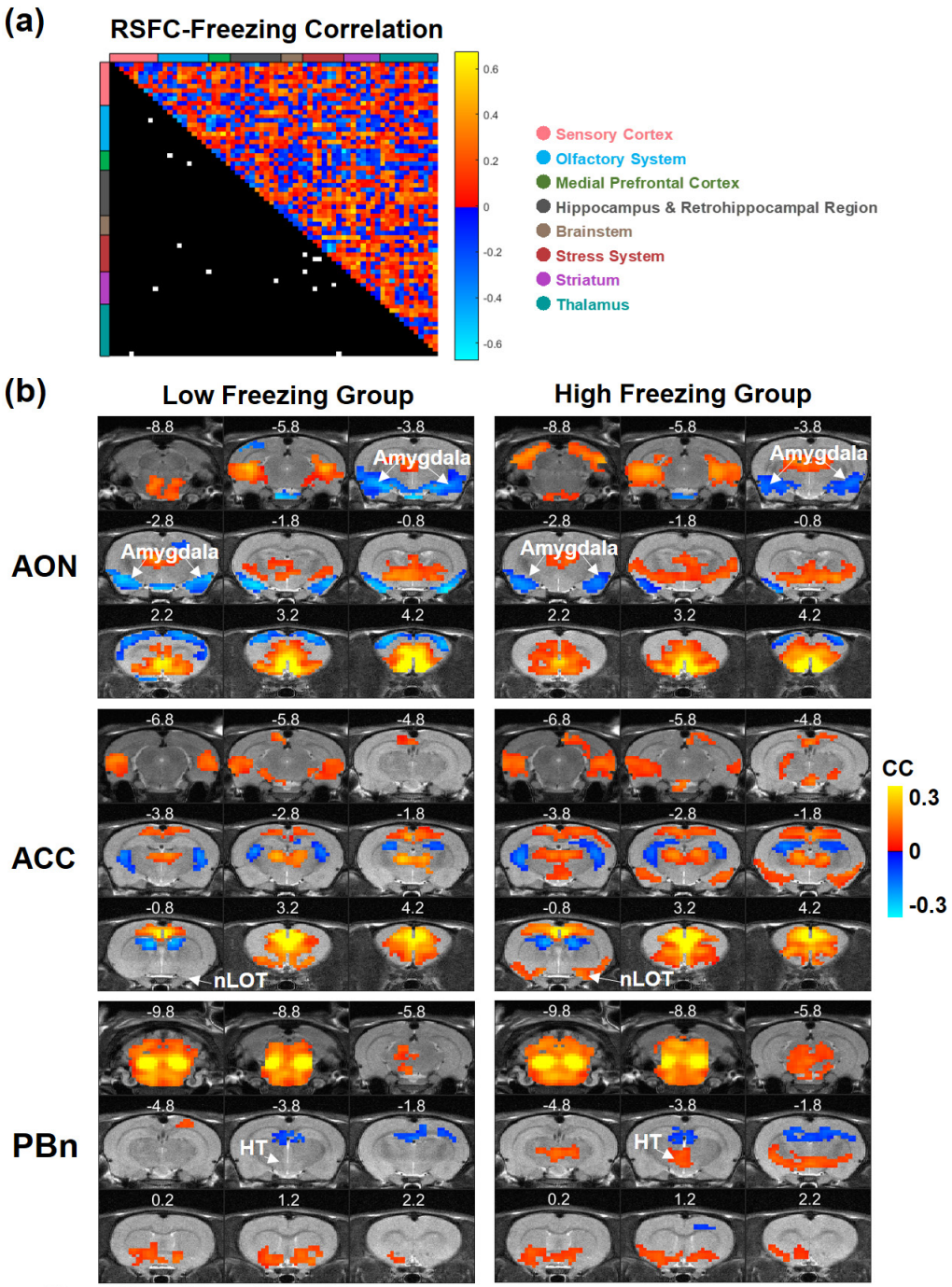

Figure 4. **a**) Correlations between pre-trauma RSFC and freezing time for all connections (upper triangle) and super-threshold connections (lower triangle, each white element represents a super-threshold connection). Brain regions are arranged based on the brain system (color coded) they belong to. **b**) Three representative RSFC maps, generated with ACC, AON and PBn as the seed, respectively (colored voxels, $p < 0.05$, FDR corrected). Distance to Bregma was labeled at the top of each slice. ACC, anterior cingulate cortex; AON, anterior olfactory nucleus; HT, hypothalamus; nLOT, lateral olfactory tract nucleus; PBn, parabrachial nucleus.

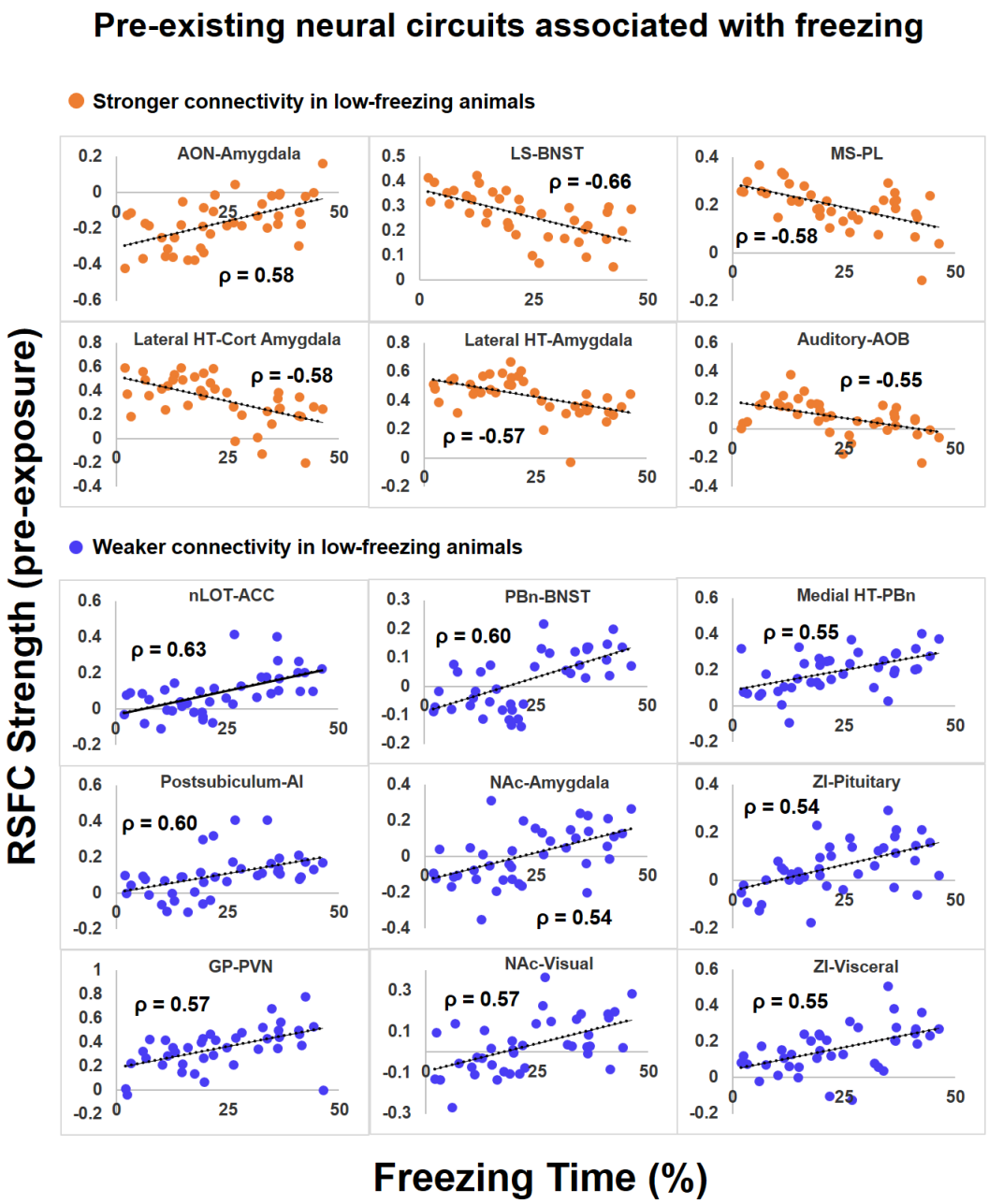

Figure 5. Neural circuits with pre-trauma resting-state functional connectivity (y-axis) correlated ($p<0.05$, FDR corrected) with percentage freezing time (x-axis) in all fox urine exposed animals (n=62). AON, anterior olfactory nucleus; LS, lateral septum; BNST, bed nucleus of the stria terminalis; MS, medial septum; PL, prelimbic cortex; HT, hypothalamus; Cort Amygdala, cortical amygdala; AOB, accessory olfactory Bulb; nLOT, lateral olfactory tract nucleus; ACC, anterior cingulate cortex; PBn, parabrachial nucleus; AI, postsubiculum-agranular insula; NAc, nucleus accumbens; ZI, zona inserta; GP, globus pallidus; PVN, paraventricular nucleus.

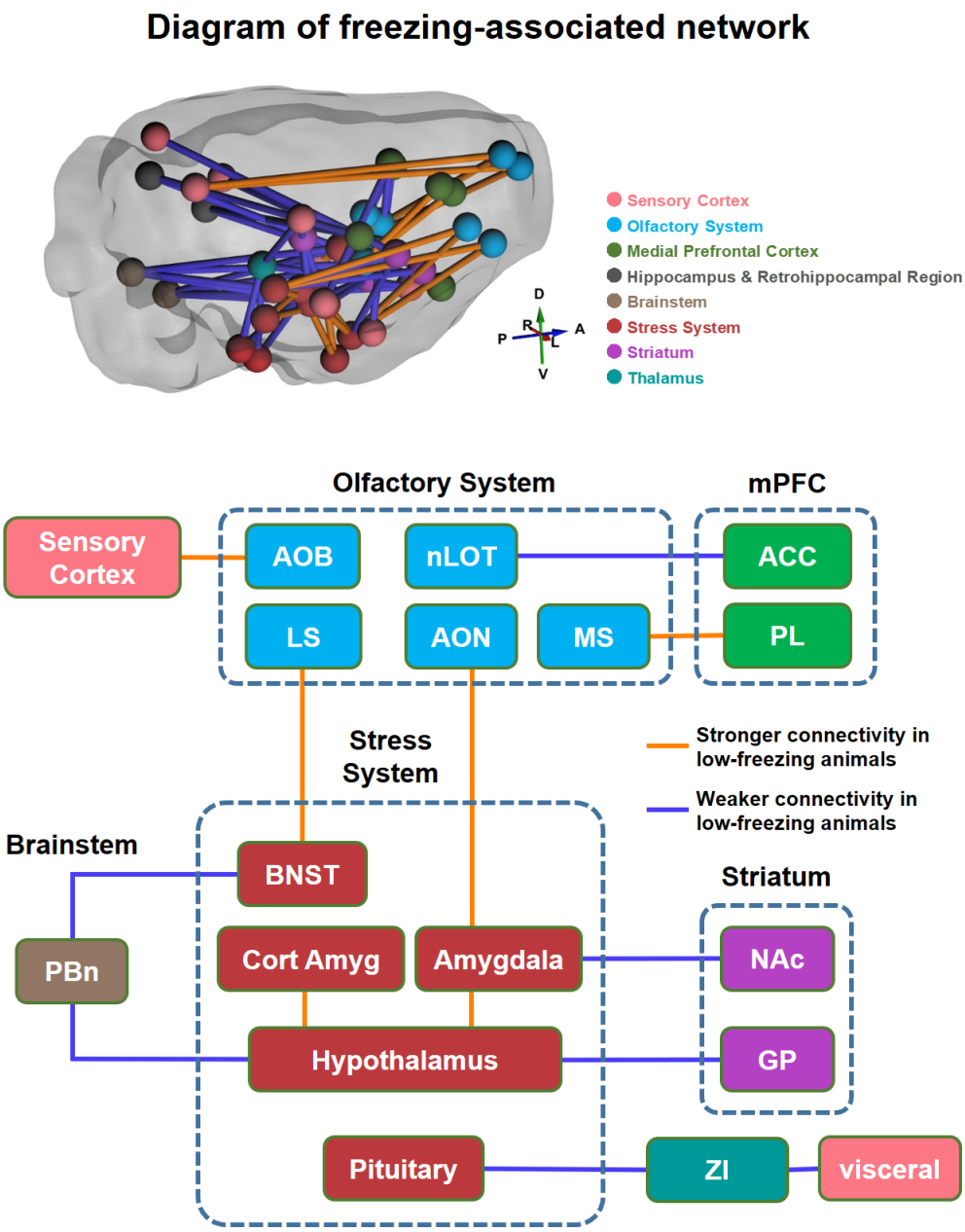

Figure 6. Diagram of freezing-associated neural network, including neural circuits showing significant correlation between pre-trauma RSFC and total freezing time shown in Fig. 5. Brain regions are grouped and color coded based on the brain systems they belong to. Orange lines indicate stronger connectivity in low-freezing animals. Blue lines indicate weaker connectivity in low-freezing animals. See the caption of Fig. 5 for the abbreviation.